(4-Piperidinyl)-piperazine: A new platform for acetyl-CoA carboxylase inhibitors

Tomomichi Chonan [a,*], Takahiro Oi [a], Daisuke Yamamoto [b], Miyoko Yashiro [c], Daisuke Wakasugi [a], Hiroaki Tanaka [a], Ayumi Ohoka-Sugita [b], Fusayo Io [b], Hiroko Koretsune [b], Akira Hiratate [a]

[a] Medicinal Chemistry Laboratories, Taisho Pharmaceutical Co., Ltd, 1-403 Yoshino-cho, Kita-ku, Saitama-shi, Saitama 331-9530, Japan
[b] Molecular Function and Pharmacology Laboratories, Taisho Pharmaceutical Co., Ltd, 1-403 Yoshino-cho, Kita-ku, Saitama-shi, Saitama 331-9530, Japan
[c] Research Computer System, Taisho Pharmaceutical Co., Ltd, 1-403 Yoshino-cho, Kita-ku, Saitama-shi, Saitama 331-9530, Japan

ABSTRACT

Acetyl-CoA carboxylases (ACCs), the rate limiting enzymes in de novo lipid synthesis, play important roles in modulating energy metabolism. The inhibition of ACC has demonstrated promising therapeutic potential for treating obesity and type 2 diabetes mellitus in transgenic mice and preclinical animal models. We describe herein the synthesis and structure–activity relationships of a series of disubstituted (4-piperidinyl)-piperazine derivatives as a new platform for ACC1/2 non-selective inhibitors.

© 2009 Elsevier Ltd. All rights reserved.

Acetyl-CoA carboxylase (ACC) is a biotin-dependent homo oligomeric protein composed of a carboxyltransferase (CT), a biotin carboxyl carrier protein and biotin carboxylase (BC) domains. ACC is involved in the synthesis of malonyl-CoA from acetyl-CoA in an ATP-dependent manner. Malonyl-CoA works not only as a substrate for de novo fatty acid synthesis, but also as an allosteric inhibitor of carnitine palmitoyl transferase (CPT-1), a key enzyme that positively regulates mitochondrial β-oxidation. Therefore, inhibition of ACC is expected to reduce de novo fatty acid synthesis (FAS) and to enhance fatty acid β-oxidation (FAO) through disinhibition of CPT-1, which might benefit treatment of metabolic disorders such as obesity and diabetes.[1]

Two ACC isoforms, ACC1 and ACC2, have been cloned in rodents and humans. ACC1 is predominantly expressed in lipogenic tissues such as liver and adipose tissue, while ACC2 is predominantly expressed in oxidative tissues such as liver, skeletal muscle and heart.[2] Consequently, reduction of malonyl-CoA levels in these tissues by ACC1/2 non-selective inhibitors is expected to reduce de novo fatty acid synthesis and triglyceride (TG)-rich lipoprotein secretion in liver, while increasing fatty acid β-oxidation in liver and skeletal muscle. Therefore, an ACC1/2 non-selective inhibitor might provide a novel therapeutic approach for treating various metabolic disorders.

We have initiated a drug discovery program directed towards the identification of potent ACC inhibitors with appreciable metabolic stability based on CP-640186 (Fig. 1), a non-selective inhibitor of ACC 1 and 2 (rat ACC1 IC_{50} = 53 nM, rat ACC2 IC_{50} = 61 nM).[1]

In order to enhance the intrinsic potency of CP-640186, the introduction of a new central core structure was deemed essential. For this purpose, we screened our scaffold collections and identified a (4-piperidinyl)-piperazine class of compound **1** with an IC_{50} of 239 nM, which appeared to be a potential lead structure for further optimization. The metabolic stability of compound **1** was assessed using a human microsomal incubation assay; only 19% of the intact compound was recovered,[3] indicating that compound **1** is metabolically unstable. A metabolite identification study of **1** revealed that the left-hand anthranyl and the right-hand morpholyl groups are the main sites metabolized. Having identified potential lead **1**, we initiated detailed SAR studies.
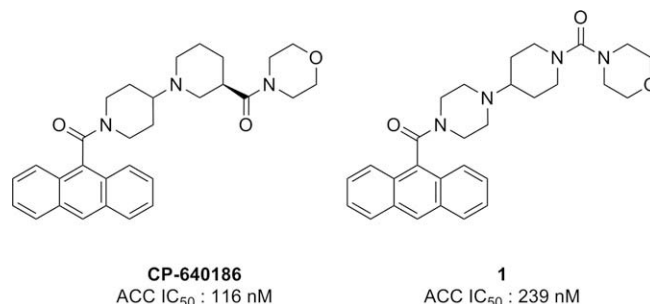

CP-640186
ACC IC_{50} : 116 nM
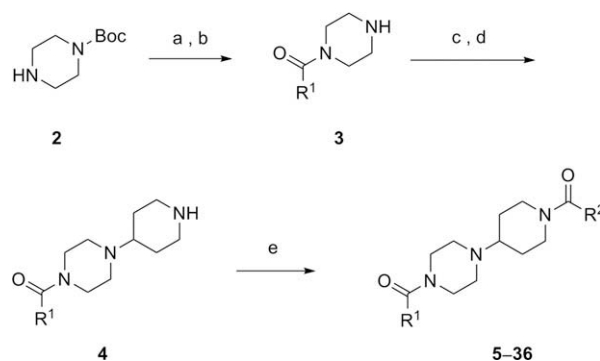
1
ACC IC_{50} : 239 nM

Figure 1. CP-640186 and compound **1**.

* Corresponding author. Tel.: +81 48 669 3108; fax: +81 48 652 7254.
E-mail address: tomomichi.chonan@po.rd.taisho.co.jp (T. Chonan).

The co-crystal structure of CP-640186 and yeast ACC has been reported by Zhang et al.[4] CP-640186 tightly associates with the active site of the carboxyltransferase (CT) domain of yeast ACC and blocks the binding of the biotin substrate to the CT domain at the domain's dimer interface. The crystal structure shows that the oxygen of the anthranyl amide of CP-640186 is hydrogen-bonded to the main chain amide of Glu2026′ near the beginning of helix α6, whereas the carbonyl oxygen adjacent to the morpholine is hydrogen-bonded to the main chain amide of Gly1958′. Given that the amino acid sequence of the active site of the CT domain is highly conserved across eukaryotic species having multi-domain ACCs,[5] modeling studies were carried out using MOE.[6] The homology model of the CT domain of human ACC2 from the crystal structure of yeast ACC in complex with CP-640186 (PDB ID: 1W2X) was used. The predicted binding mode of compound 1 (in yellow) is shown in Figure 2, along with an overlay of CP-640186 (in purple). The predicted binding mode suggests that the carbonyl oxygen of the morpholinyl amide of 1 is not hydrogen-bonded to Gly2162′ (yeast Gly1958′); nevertheless, the morpholine rings of both CP-640186 and compound 1 occupy the same pocket.

The general synthesis of the substituted (4-piperidinyl)-piperazine analogues is outlined in Scheme 1. tert-Butoxy piperazine-1-carboxylate (2) was coupled with the desired acid chloride under basic conditions, followed by removal of the tert-butoxycarbonyl (Boc) group to give the substituted piperazine 3. The amino group of 3 was reductively alkylated with tert-butyl 4-oxopiperidine-1-carboxylate followed by cleavage of the Boc group to afford 4, which was coupled with the desired acid chloride or carboxylic acid to give the target compounds 5–36.

The derivatives were screened against partially purified human liver ACC enzymes, and the subtype selectivity of the optimized compounds was confirmed using recombinant human ACC1 and ACC2 enzymes. Among the tested compounds, the selected potent compounds were further evaluated for their ability to decrease fatty acid synthesis (FAS) and increase fatty acid oxidation (FAO) in HepG2 cells. FAS inhibition was assessed by measuring the de-

crease in [^{14}C] acetate incorporation into cellular lipids,[1a] and the effects on FAO were evaluated by measuring the generation of T_2O in the culture media.[7]

The right-hand piperidine substituent was modified initially (compound 5–11, Table 1). The piperidyl, cyclohexyl, and cyclopentyl derivatives (5, 8, and 9) showed slightly increased activity. The benzyl derivative 7 displayed a substantial decrease in potency. The phenyl and 3-(2,5-dimethylfuryl) derivatives (6 and 11) showed improved potency compared to the parent compound 1. Next, the metabolically labile anthranyl group was replaced by a (2,6-diphenyl)pyridyl group[8] (12–18, Table 1). The (2,6-diphenyl)pyridyl

Scheme 1. Reagents and conditions: (a) R^{1}COCl, Et$_3$N, CHCl$_3$, rt; (b) 4 M HCl–AcOEt, MeOH, rt; (c) 1-Boc-piperidone, CHCl$_3$, rt, then NaBH(OAc)$_3$, CHCl$_3$, rt; (d) 4 M HCl–AcOEt, MeOH, rt; (e) (i) R^{2}COOH, EDCl, HOBt, Et$_3$N, DMF, rt, or R^{2}COCl, Et$_3$N, CHCl$_3$, (ii) 4 M HCl–AcOEt, or 1 M maleic acid in AcOEt.

Table 1
In vitro ACC activity and metabolic stability in human liver microsomes of the disubstituted (4-piperidinyl)-piperazines 1, 5–18

Compd	R^1	R^2	ACC IC$_{50}$[a] (nM)	hMS[b] (%)
1	9-Anthranyl	4-Morpholinyl	239	19
5	9-Anthranyl	1-Piperidyl	121	ND[c]
6	9-Anthranyl	Phenyl	66	ND[c]
7	9-Anthranyl	Benzyl	2112	ND[c]
8	9-Anthranyl	Cyclohexyl	91	ND[c]
9	9-Anthranyl	Cyclopentyl	95	ND[c]
10	9-Anthranyl	2-Furyl	161	ND[c]
11	9-Anthranyl	3-(2,5-Dimethylfuryl)	60	ND[c]
12	4-(2,6-Diphenyl)-pyridyl	4-Morpholinyl	869	ND[c]
13	4-(2,6-Diphenyl)-pyridyl	1-Piperidyl	434	ND[c]
14	4-(2,6-Diphenyl)-pyridyl	Phenyl	693	96
15	4-(2,6-Diphenyl)-pyridyl	Cyclohexyl	244	61
16	4-(2,6-Diphenyl)-pyridyl	3-(2,5-Dimethylfuryl)	157	37
17	4-(2,6-Diphenyl)-pyridyl	1-Acetylpiperidin-4-yl	126	79
18	4-(2,6-Diphenyl)-pyridyl	trans-4-Methoxy-cyclohexyl	155	52

[a] Inhibitory activity of compounds on the malonyl-CoA synthesis of human ACC1/2.
[b] % Remaining after 15-min incubation with human liver microsomes (1 mg protein/mL).
[c] No data.
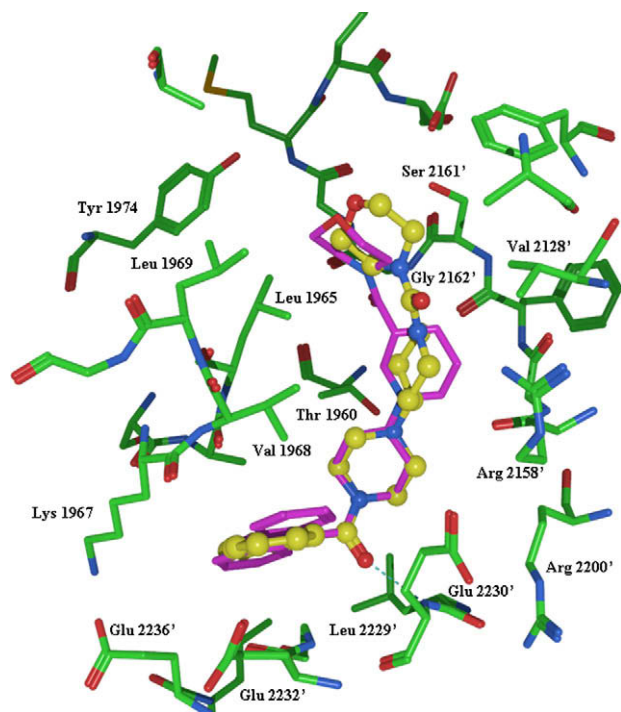
Figure 2. Optimized binding mode of 1.

derivatives were found to be substantially less potent than the corresponding anthranyl derivatives. Of them, compounds **16**–**18** displayed appreciable activity. We speculate that the enhanced activity of **16**–**18** is partly due to their interaction with Tyr1974 (Fig. 2). A molecular model of compound **17** (in yellow) is shown in Figure 3 along with an overlay of CP-640186 (in purple). The predicted binding mode suggests that the diphenyl pyridine moiety of **17** is trapped in a narrow space where the anthranyl group of CP-640186 resides, and the adjacent carbonyl group hydrogen-bonds to the main chain amide of Glu2230′ (yeast Glu2026′). The left-hand 1-acetylpiperidine moiety of **17** fits into the mostly hydrophobic area on the surface of the active site, and the acetyl group of the piperidine is capable of binding to Tyr1974. In addition to good activity, the potent (2,6-diphenyl) pyridyl derivative **17** was found to have good microsomal stability (Table 1).

Optimization of the acetyl substituent of **17** was attempted (Table 2). The benzamide **20**, isopropyl carbamate **24** and methane sulfonamide **28** were substantially less potent than compound **17**, showing that bulky substituents tend to decrease ACC inhibitory potency. No compounds with noticeably improved characteristics were identified by this limited modification study.

Finally, substituent effects on the left-hand side phenyl groups were investigated (Table 3). The fluoro derivatives **29** and **30** were less potent than the parent **17**. The methyl **31** and methoxy **32** derivatives exhibited improved ACC inhibitory activity both in enzyme and cell-based assays. The 4-hydroxymethyl derivative **34** displayed the most potent enzyme activity among this series, with an IC$_{50}$ value of 32 nM; nevertheless, its cell activity was substantially lower than those of **31** and **32**, probably due to their limited cell permeability. Also the 4-hydroxyl derivative **33** and the 3- and 4-aminocarbonyl derivatives **35** and **36** exhibited significantly reduced enzymatic activity in cells, probably for the same reason. The metabolic stability of derivatives **29**–**32** were improved compared to compound **17**. Derivative **31**, which has optimal activity in the FAS and FAO cell assays, was selected for further pharmacological profiling.

The pharmacological profiles of **31** are summarized in Table 4. Compound **31** displayed more potent activity against human re-
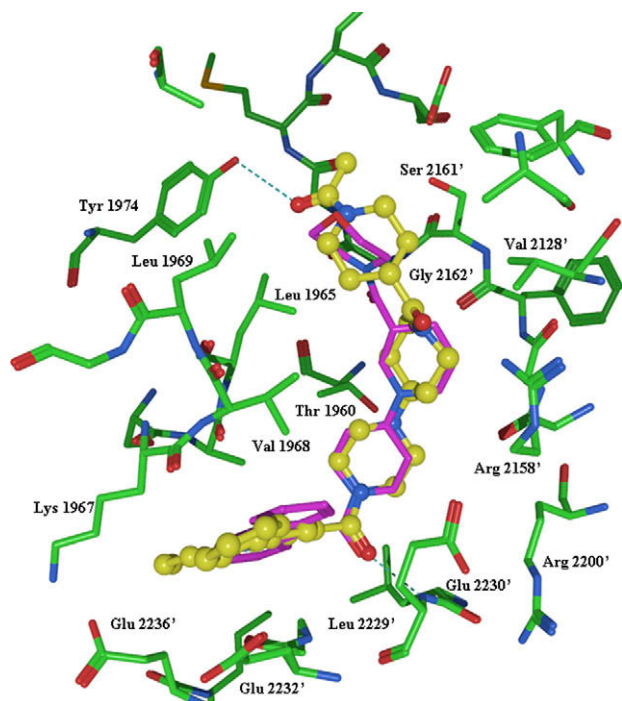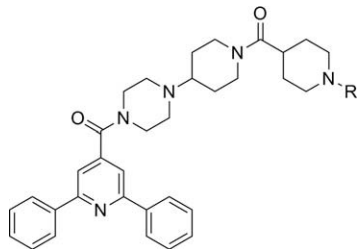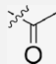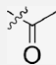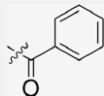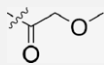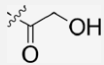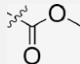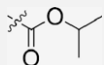

Figure 3. Optimized binding mode of **17**.

Table 2
In vitro activities of the disubstituted 4-(4-piperidinyl)-piperazines **17**, **19**–**28**

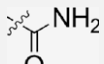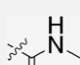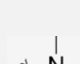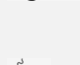| Compd	R	ACC IC$_{50}$[a] (nM)
17	(acetyl)	126
19	(propionyl)	115
20	(benzoyl)	290
21	(methoxyacetyl)	169
22	(hydroxyacetyl)	102
23	(methoxycarbonyl)	102
24	(isopropoxycarbonyl)	411
25	(aminocarbonyl)	151
26	(N-methylaminocarbonyl)	95
27	(N,N-dimethylaminocarbonyl)	169
28	(methanesulfonyl)	248

[a] Inhibitory activity of compounds on malonyl-CoA synthesis of human ACC1/2.

combinant ACC2 (rhACC2) than human recombinant ACC1 (rhACC1).[9] In HepG2 cell assays, compound **31** showed dose-dependent inhibition of fatty acid synthesis, with an IC$_{50}$ of

Table 3
In vitro activities of the disubstituted 4-(4-piperidinyl)-piperazine **17**, **29–36**
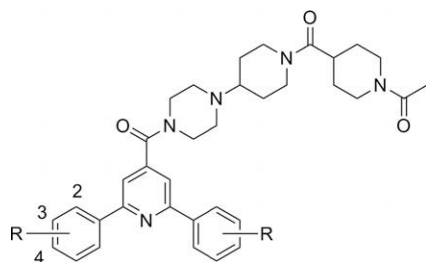
Compd	R	ACC IC$_{50}$[a] (nM)	FAO[b] (%)	FAS[c] (%)	hMS[d] (%)
17	H	126	148	72	79
29	3-F	131	ND[e]	ND[e]	90
30	4-F	184	ND[e]	ND[e]	94
31	4-Me	76	176	77	87
32	4-OMe	68	167	77	87
33	4-OH	52	123[f]	29[f]	ND[e]
34	4-CH$_2$OH	32	120[f]	ND[e]	ND[e]
35	3-CONH$_2$	73	94[f]	ND[e]	ND[e]
36	4-CONH$_2$	67	135[f]	ND[e]	ND[e]

[a] Inhibitory activity of compounds on malonyl-CoA synthesis of human ACC1/2.
[b] Activation of fatty acid oxidation in HepG2 cells at 1 μM.
[c] Inhibitory activity of fatty acid synthesis in HepG2 cells at 1 μM.
[d] % Remaining after 15-min incubation with human liver microsomes (1 mg protein/mL).
[e] No data.
[f] Screening concentration at 10 μM.

Table 4
Pharmacological profiles and plasma exposure of **31** and CP-640186

Pharmacological profiles	**31**	CP-640186
Enzyme assay[a]		
hACC 1/2	76 nM	116 nM
rhACC1	101 nM	456 nM
rhACC2	23 nM	194 nM
Cell-based assay		
HepG2 Cell FAS (IC$_{50}$)	0.34 μM	0.84 μM
HepG2 Cell FAO (EC$_{50}$)	0.58 μM	ND[b]
Microsomal metabolism[c]		
Human liver microsomes	87	52
Rat liver microsomes	96	ND[b]
Plasma exposure after po[d]		
C_{max} (ng/mL)	107	ND[b]
T_{max} (h)	4.00	ND[b]
AUC (ng/mL h)	1000	ND[b]

[a] Inhibitory activity of compounds on the malonyl-CoA synthesis of human ACC1/2, recombinant hACC1 and hACC2.
[b] No data.
[c] % Remaining after 15-min incubation with human liver microsomes (1 mg protein/mL).
[d] Plasma exposure after single oral administration of **31** at a dose of 10 mg/kg to male Sprague-Dawley rats.

0.34 μM, and caused an increase in fatty acid oxidation, with an EC$_{50}$ of 0.58 μM. Additionally, compound **31** is metabolically stable in human and rat liver microsomes and showed no significant inhibitory effects on the major cytochrome P450 isozymes (CYP1A2, CYP2C9, CYP2C19, CYP2D6, and CYP3A4).

In conclusion, we have identified the (4-piperidinyl)-piperazine scaffold as a new platform for ACC1/2 non-selective inhibitors and discovered compound **31**, which has promising activity. Compound **31** exhibited significantly improved metabolic stability in liver microsomes as compared with the lead compound **1**. Further modification of this series is ongoing in order to improve ACC inhibitory potency.

Acknowledgments

Supplementary data

Supplementary data associated with this article can be found, in the online version, at doi:10.1016/j.bmcl.2009.10.012.

References and notes

1. (a) Harwood, H. J., Jr.; Petras, S. F.; Shelly, L. D.; Zaccaro, L. M.; Perry, D. A.; Makowski, M. R.; Hargrove, D. M.; Martin, K. A.; Tracey, W. R.; Chapman, J. G.; Magee, W. P.; Dalvie, D. K.; Soliman, V. F.; Martin, W. H.; Mularski, C. J.; Eisenbeis, S. A. *J. Biol. Chem.* **2003**, *278*, 37099; (b) Harwood, H. J., Jr. *Exp. Opin. Cardiovasc. Renal.* **2005**, *9*, 267; (c) Corbett, J. W.; Harwood, H. J., Jr. *Rec. Pat. Cardiovasc. Drug Discovery* **2007**, *2*, 162.
2. Abu-Elheiga, L.; Matzuk, M. M.; Abo-Hashema, K. A.; Wakil, S. J. *Science* **2001**, *291*, 2613.
3. *Metabolic stability in liver microsomes*: 5 μM compound was incubated at 37 °C in 1 mg/mL human or rat microsomes supplemented with 1.5 mM glucose-6-phosphate, 0.16 mM β-nicotinamide-adenine dinucleotide phosphate, 1 U/mL glucose-6-phosphate dehydrogenase, 250 mM phosphate buffer, 2.4 mM magnesium chloride and 69 mM potassium chloride. Concentrations of the test compound were determined by LC–MS/MS. Metabolic stability was calculated from the ratio of the test compound concentration at 0 min to its concentration after15-min incubation.
4. Zhang, H.; Tweel, B.; Li, J.; Tong, L. *Structure* **2004**, *12*, 1683.
5. Tong, L. *Cell. Mol. Life Sci.* **2005**, *62*, 1784.
6. MOE (Molecular Operating Environment); Chemical Computing Group: Montreal, Quebec, Canada, 2006.
7. Anne, M.; William, J. R. *J. Clin. Invest.* **1987**, *79*, 59.
8. Shinde, P.; Srivastava, S. K.; Odedara, R.; Tuli, D.; Munshi, S.; Patel, J.; Zambad, S. P.; Sonawane, R.; Gupta, R. C.; Chauthaiwale, V.; Dutt, C. *Bioorg. Med. Chem. Lett.* **2009**, *19*, 949.
9. Dong, C.; Ching-Hsuen, C.; Luping, C.; John, N. F.; Gabe, A. M.; Yuli, W.; Joseph, W. C.; Mark, R. H.; Gregory, A. L.; Yongmi, A.; James, K. T. *Protein Exp. Purif.* **2007**, *51*, 11.